Journal of Engineering and Applied Science

Publishing model: **Open access**

Articles

Search all Journal of Engineering and Applied Science articles →

Filter by

Volume:

Volume 73 (2026)

Publishing model:

☐ Open access only

Sort by

Date published:

New to old Old to new

Update results

Showing 1–50 of 151 articles

Adaptive LIPM-based trajectory planning for energy-efficient bipedal locomotion on inclined terrains

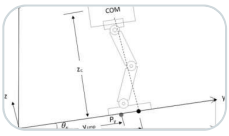

Research | Open access | 21 April 2026 | Article: 151

Numerical and parametric analysis of built-up cold-formed steel battened beam-columns under axial and eccentric loading

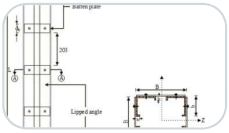

Research | Open access | 21 April 2026 | Article: 150

Renewable generation expansion planning for Ecuador's coastal region: a stochastic optimisation approach

Research | Open access | 20 April 2026 | Article: 149

Ultra-low-frequency piezoelectric energy harvesting via adjustable nonlinear inertance

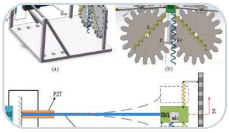

Research | Open access | 20 April 2026 | Article: 148

Transformer partial discharge fault waveform recognition method based on MDW-YOLO

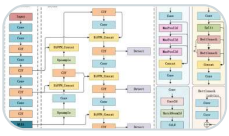

Research | Open access | 20 April 2026 | Article: 147

Multi-lane line detection algorithm based on feature point instance segmentation

Research | Open access | 20 April 2026 | Article: 146

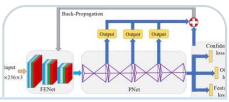

Correction: Rapid coconut shell charcoal briquette drying completion determinant using plate electrodes with electrolyte

Correction | Open access | 17 April 2026 | Article: 145

Powerful deep convolutional neural networks for robust automatic modulation classification using spectrograms

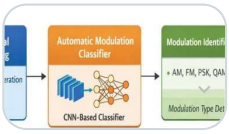

Research | Open access | 17 April 2026 | Article: 144

Research and development of gold mine paste filling materials in the Dandong region and their role in controlling abandoned mine area stability and surface subsidence

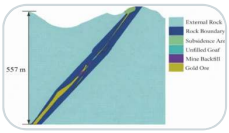

Research | Open access | 17 April 2026 | Article: 143

Predicting slug liquid holdup in a two-phase gas–liquid vertical flow

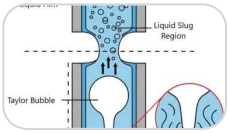

Research | Open access | 16 April 2026 | Article: 142

Ultrasound-assisted adsorption of congo red dye using green synthesized silver nanoparticles coated with chitosan

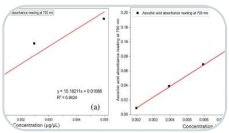

Research | Open access | 15 April 2026 | Article: 141

Enhancing performance of lightweight electric vehicles through advanced speed control of BLDC motors

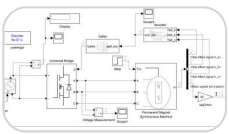

Research | Open access | 14 April 2026 | Article: 140

Correction: Post fire performance of interior two-way RC beam to column joint strengthened with CFRP sheets subjected to cyclic loading

Correction | Open access | 14 April 2026 | Article: 139

Study of the interference factors and defect temperature field characteristics of infrared testing for composite insulators

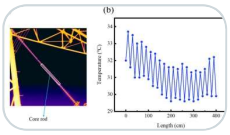

Research | Open access | 14 April 2026 | Article: 138

A climate-adaptive thermo-mechanical mathematical model for predicting cumulative creep damage in gas turbine blades

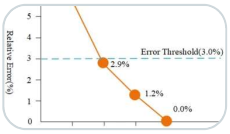

Research | Open access | 14 April 2026 | Article: 137

Experimental evaluation of mechanical, tribological, and morphological characteristics of alkali-treated pineapple leaf fiber reinforced epoxy composites for structural and biomedical applications

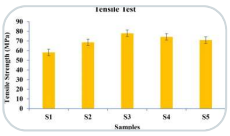

Research | Open access | 14 April 2026 | Article: 136

A comparative study of detectors, descriptors, and matching techniques for real-time object tracking in autonomous driving: balancing performance, robustness, and energy efficiency

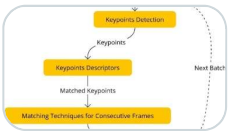

Research | Open access | 11 April 2026 | Article: 135

A novel end-to-end dual-branch model for fault diagnosis of motor bearings based on cross-domain semantic pattern fusion

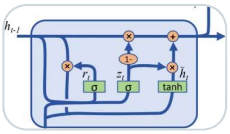

Research | Open access | 09 April 2026 | Article: 134

PiST-Net: a physics-informed spatiotemporal framework for low-voltage distribution grid topology inference

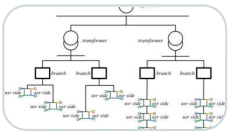

Research | Open access | 09 April 2026 | Article: 133

Performance comparison of rectangular mini-channel and conventional round tube condensers in split-type air conditioning system: an experimental approach

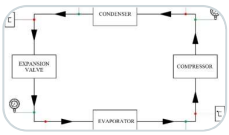

Research | Open access | 08 April 2026 | Article: 132

Influence of joint roughness on the evolution of shear–seepage characteristics of granite

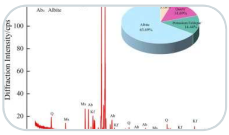

Research | Open access | 06 April 2026 | Article: 131

Study of tribological and corrosion behavior of AA6061–SiC–WS_2/WSe_2 hybrid composites using the taguchi method

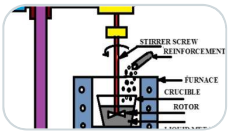

Research | Open access | 02 April 2026 | Article: 130

Multimodal traffic flow analysis and congestion prediction on expressways: evaluating the importance of machine learning models and features for improving prediction accuracy in urban traffic management

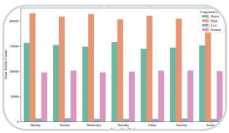

Research | Open access | 02 April 2026 | Article: 129

Influence of mineral and organic acids on the structural, morphological and packing properties of silica sand

Research | Open access | 01 April 2026 | Article: 128

Hercynite pinning delivers enhanced creep resistance in Fe_2O_3–reinforced Al6061: experiments and Arrhenius modeling

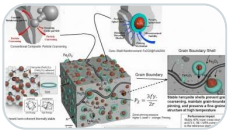

Research | Open access | 31 March 2026 | Article: 127

Bio-based and regenerative materials in interior design: a systematic literature review and bibliometric analysis

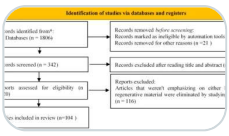

Reviews | Open access | 30 March 2026 | Article: 126

An adaptive deep reinforcement learning framework enhanced by broad reinforcement learning–based state transition for efficient task offloading and resource allocation at the network edge

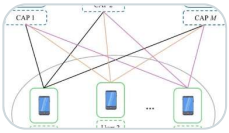

Research | Open access | 27 March 2026 | Article: 125

Optimizing ANFIS for heating load forecasting: a hybrid approach for enhanced accuracy in district heating systems

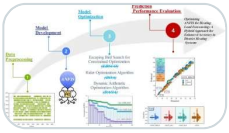

Research | Open access | 25 March 2026 | Article: 124

Design and implementation of a machine learning-integrated reliable quality control evaluation system for cigarette manufacturing process

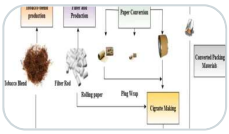

Research | Open access | 25 March 2026 | Article: 123

Investigation of plunge depth and tool geometry effects on the mechanical properties and microstructure of dissimilar AZ31B-AA1100 Micro Friction Stir Spot Welding (mFSSW)

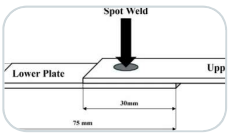

Research | Open access | 25 March 2026 | Article: 122

Statistical approach on aging characteristic of buton rock asphalt modified by nanoadditives

Research | Open access | 24 March 2026 | Article: 121

Spatial optimization methods for waste-to-energy facility siting: a review of GIS-MCDA approaches

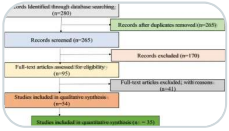

Reviews | Open access | 20 March 2026 | Article: 120

Multi-agent for analyzing power outage causes in distribution networks of new power system

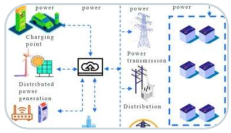

Research | Open access | 19 March 2026 | Article: 119

Improvement of bearing capacity of shallow foundations with cemented sand as replacement layer

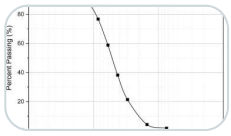

Research | Open access | 19 March 2026 | Article: 118

Improved YOLOv11-based algorithm for identifying birds intruding on power lines

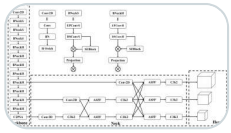

Research | Open access | 19 March 2026 | Article: 117

Rapid coconut shell charcoal briquette drying completion determinant using plate electrodes with electrolyte

Research | Open access | 19 March 2026 | Article: 116

Finite element based comparative analysis of damage in an anti-underrun device via contact simulation and quasi-static procedure

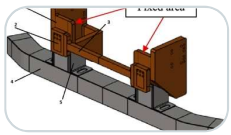

Research | Open access | 18 March 2026 | Article: 115

New predictive methodology for severity assessment of corrosion and gouge defects in pipelines

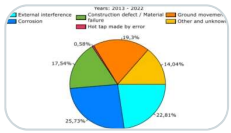

Research | Open access | 18 March 2026 | Article: 114

Modelling of tensile strength of 3D printed PETg, ABS and ASA based novel filament

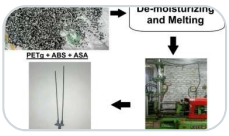

Research | Open access | 18 March 2026 | Article: 113

Towards sustainable grid security: a lightweight adaptive framework for power system software vulnerability detection

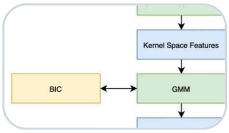

Research | Open access | 17 March 2026 | Article: 112

Dynamic prediction model for coal mine roof disasters based on spatiotemporal graph neural network

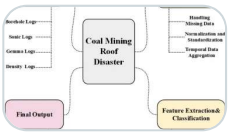

Research | Open access | 17 March 2026 | Article: 111

Experimental assessment of acid gas energy recovery potential in refinery operations

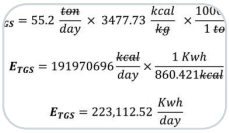

Research | Open access | 17 March 2026 | Article: 110

Comparative structural evaluation of polymer-based morphing wing ribs using finite element analysis for optimized adaptive aerospace applications

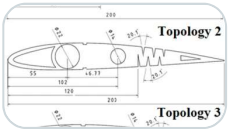

Research | Open access | 16 March 2026 | Article: 109

Optimising complex systems: model predictive control in engineering applications

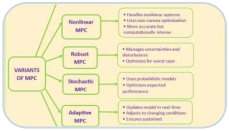

Reviews | Open access | 16 March 2026 | Article: 108

Crack detection and semantic segmentation in concrete structures using an improved deep learning-based framework

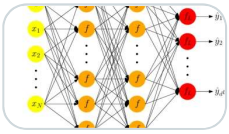

Research | Open access | 14 March 2026 | Article: 107

A comprehensive review on H-type Darrieus wind turbine: aerodynamics, blade profile, CFD simulations

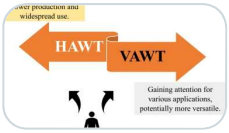

Reviews | Open access | 14 March 2026 | Article: 106

STDP learning in saturated differential amplifier circuits: design and analysis

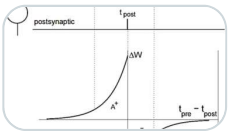

Research | Open access | 12 March 2026 | Article: 105

A three-dimensional vision-based method for weak-texture defect detection and precise measurement in electrical automation manufacturing

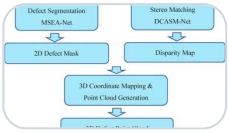

Research | Open access | 11 March 2026 | Article: 104

Post-impact response of rectangular hollow steel tubes: comparative study on partially and fully concrete-filled columns

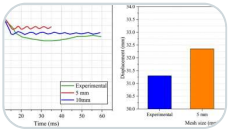

Research | Open access | 11 March 2026 | Article: 103

A method for detecting abnormal heating in switchgear based on SAHDA

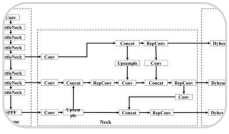

Research | Open access | 10 March 2026 | Article: 102

Prasetyadi *et al. Journal of Engineering and Applied Science* (2026) 73:116
https://doi.org/10.1186/s44147-026-00976-x

Journal of Engineering and Applied Science

RESEARCH Open Access

Rapid coconut shell charcoal briquette drying completion determinant using plate electrodes with electrolyte

Andreas Prasetyadi[1*], Bernadeta Wuri Harini[2] and Rusdi Sambada[1]

*Correspondence:
Andreas Prasetyadi
pras@usd.ac.id
[1]Mechanical Engineering Department, Faculty of Science and Engineering, Universitas Sanata Dharma, Yogyakarta 55282, Indonesia
[2]Electrical Engineering Department, Faculty of Science and Engineering, Universitas Sanata Dharma, Yogyakarta 55282, Indonesia

Abstract

Drying completion determinant is critical in coconut charcoal briquette production due to both cost and quality concerns. To address this, research was conducted to determine the drying level of briquettes using resistivity measurements with plate electrodes and electrolytes. The study aimed at finding the possibility of applying combination of plate electrodes and electrolytes for rapid determination of stopping the drying process in coconut shell charcoal briquette production. In this study, two distinct methods were performed: the direct approach and the indirect approach. On one hand, the direct method applied Ohm's Law to current and voltage data. On the other hand, the indirect method utilized a voltage divider approach to calculate resistivity. Both methods were conducted to test the cube-shaped briquettes (2.5 cm per side) with moisture content (MC) levels ranging from 4% to 16%. The direct method provided results close to rod electrodes. Meanwhile, the indirect approach provided very precise results with deviation standard less than 1.5%. The resistivity of the threshold of market acceptable briquette was above 10 kohm.m for moisture content less than 5%. These findings indicate a clear distinction between wet and dry briquettes, demonstrating the possibility of applying the instrumentation of a fast stop drying determinant. The indirect method can reduce decision time and fuel cost by 5%.

Keywords Briquette quality instrumentation, Briquette mass, Briquette resistivity, Drying time, Moisture content prediction

Introduction

Briquettes are a solid fuel widely considered a prospective green and clean one. These two atributes refer to the emission and toxicity level of the fuel [1]. A green fuel has a low carbon footprint characterized by carbon dioxide released and adsorbed along the fuel life cycle, while the cleanness of the briquette is related to its quality. A briquette can be produced from biomass waste [2, 3] or any biomass from special plants for briquettes [2, 4, 5] with additional material as the binder. Briquettes are typically produced from bamboo [6], groundnut [7–9], husk [10], sawdust [11], any charcoal [2, 6, 12], and coal [13]. Research has been conducted to understand many aspects of the briquette quality

[14–18], briquette production [15, 18–20], and other aspects of its lifecycle processes [21, 22]. Among the research on the briquette quality, physical parameters are studied alongside the chemical ones. In particular, density, hardness, burning rate, and moisture content serve as the primary physical parameters of the briquette quality [5, 16, 23, 24].

Of those parameters, moisture content is the important physical parameter of the briquette quality, along with agglomeration. A good charcoal briquette is required to have a moisture content below 8% in Indonesia, Japan, and some other countries [13, 25]. A European Wood Pellet Product standard (ENPlus) requires the moisture content of the biomass fuel briquettes below 10% [25]. The moisture content implies the calorific value of a briquette [26]. According to the proximity approach, every percent of moisture content in a briquette is equivalent to 78 cal/g [27]. The necessary energy for evaporating the moisture content affects the heating value of a fuel and its mass. Therefore, the moisture content also affects briquette density [28]. Consequently, higher moisture content results in less available energy for harnessable combustion [24, 29]. In 2013, Gebreegziabher et al. reported that the lower heating value (LHV) of a wood chip with 43% moisture content was less than the LHV of the chips with 17% moisture content by more than one third. The LHV of wooden chips of 0.05 m with 43% moisture content had an LHV of 9,698 kJ/kg, and those with 17% moisture content yielded 15,000 kJ/kg [30].

To produce a briquette that complies with moisture content and agglomeration, the drying process needs a specific minimum temperature. The main function of drying is to reduce the water content of the briquette. Some water was added to the mixture of matrix and binder during the blending process [13, 17, 25, 31]. Usually, a kind of thermal drying is applied to remove water content after compaction because the minimum temperature of drying is essential to create agglomeration of the charcoal powder [25]. The drying temperature affects the durability and density of briquettes. For example, heating sawdust briquettes at 130 °C was reported to create higher density briquette than heating them at 120 °C. Furthermore, the report also mentioned that 130 °C heating made a more durable sawdust briquette than 120 °C heating [4]. Meanwhile, thermal drying with a specific heat level and duration results in a variation of drying cost. Application of a higher temperature drying requires more fuel to reach the desired condition than the lower one. Accordingly, the drying duration also affects the cost of processing significantly; a longer drying duration costs more fuel. Given these costs, a rapid test to determine the drying duration is a necessity, particularly when the drying process is halted. It is reasonably important because the quality controller in a charcoal briquette factory usually conducts a burning test to ensure that the drying process is completed [28, 32]. The burning test can show different patterns of burning rate and indicate the quality of the briquettes [33, 34]. Unfortunately, a typical burning test lasting at least 120 min reveals that the decision on drying completion duration affects production cost. The fuel consumption of the burning test is 5% of the total fuel of the average briquette drying duration, taking place more than 48 h.

Resistivity has been reported as a potential drying finish determinant [28]. The study indicates that a fast and accurate determination of the drying completion could decrease the fuel cost. It has been reported, as well, that the resistivity could distinguish the cube-shaped briquettes whether they are in wet, semi-dry, or dry conditions [32]. For instance, a dry coconut shell charcoal briquette has a resistivity that is more than 1 M ohm m, while the wet one has a resistivity less than 10 k ohm m [28, 32]. Notably, the

resistivity difference of the dry and wet briquettes is more apparent than the density difference [34]. The method can also provide information on the position of the wet part inside the briquette [28]. Moreover, Prasetyadi et al. also reported that it is better than the density; the resistivity can be applied to distinguish the semi-dry charcoal briquette from the dry one [28]. However, the data shows high standard deviation of the measurement and expose the challenge of the method, which is a kind of direct method applying resistance as the measured parameter. Other charcoal electrical resistivity was reported with heat treatment for activating carbon, ranging from 15.3 milliohm m to 0.2 milliohm m at temperatures of 800 °C to 1800 °C [35]. In contrast, another report shows different results of rice straw charcoal in the order of 10^6 ohm cm [36]. The charcoal powder has a resistivity of 5 10^{-5} ohm m while the charcoal briquette is 6 10^{-5} ohm m [37].

Direct resistivity measurement using rod electrodes has been performed [28, 32]. However, it still has the drawbacks regarding precision and repetition of data acquisition. Because the briquettes have a porous surface, the contact between the electrodes and the briquette surface is unstable. Hence, skill and experience are required to measure the briquette resistivity using rod-type electrodes. Unlike the ground measurement, rod electrodes cannot be plugged into the briquette. The standard deviation of measuring resistivity using the rod electrode type was reported to be higher than 10% [28, 32]. Even though there is an exception for dry conditions, which shows the least standard deviation, it differs from the semi-dry briquette. Aforementioned, the method can also predict the position of the wet part during half-dry briquette measurement, but the variation of results remains above 5% [28]. The standard deviation phenomenon indicates that the homogeneity of the field inside the briquette is the subject of its measurement variation.

Alternatively, the plate electrode becomes a potential method to provide a homogeneous field because its construction resembles a capacitor where the electric field distributes homogeneously over the briquettes. By placing the plates on the opposite sides of the briquette and supplying different polarities, any variation of material condition between the electrodes provides a field variation. Inversely, the current between the electrodes reflects the resistivity of the material. Based on this principle, the work of Wuri Harini et al. demonstrates that the plate electrode measurement can provide an adequate and reliable trace of briquette drying conditions. The clamp application to maintain the contact between the plate electrode and the briquette surface helps this work with less resistivity difference [38]. The clamp application was also performed by [37], indicating that the contact of the plate electrodes and the briquette surface needs adjustment. Therefore, increasing the contact of the electrode and the electric charge is important.

One of the methods to increase the contact of the electrode and the surface of a porous medium is the application of an electrolyte solution, which facilitates material diffusion across the surface of the medium. Accordingly, once the electrolyte diffuses to the briquette surface, the potential difference occurs when an electric field is applied. This process implies a higher sensitivity of the medium resistivity difference. A popular application of electrolytes for increasing the contact surface is self-potential in geophysics [39]. Solution of cuprum salt is utilized as the electrolyte, in which the ion transfers the charge through a permeable membrane.

The study of measuring resistivity using plate electrodes combined with electrolyte for charcoal briquettes represents a gap that has not been studied yet. While resistivity as a method for determining moisture content is rarely performed. Moisture content, instead, is preferably measured using the density or proximity method [16, 25, 40]. The proposed study serves as the advancement of the author's previous research on the resistivity for coconut charcoal briquettes drying stop using rod electrodes [28, 32].

This work aims to investigate the applicability of the combining plate electrodes and electrolyte solution to create a rapid method of determining drying completion of the coconut shell charcoal briquette production using resistivity. The proposed method is tested by measuring the resistivity of the briquette across various conditions, ranging from 16% to 4% of moisture content. The measured resistivity of 5% moisture content is considered a critical boundary for determining the completion of the drying process. Even though it exceeds some standards, it is still an acceptable condition according to many markets. Finally, the validation of this method is demonstrated by comparing the resistivity with mass change.

The presentation of the work is structured into four distinct sections. To begin with, it is the introduction that elaborates on the significant role of the plate electrodes and electrolyte in the charcoal briquette completion determinant method. Then, the second section describes the material and elaborates on the methods covering the relevant theory, the explored briquette, the description of the experiment apparatus setup, and the procedures of measuring resistivity utilizing both direct and indirect methods. Afterward, the third section presents the results of the measurement in the previous section and the discussion about the results. At last, it is the conclusion of all the discussions in this study, underlining the resistivity of the briquette with a moisture content of less than 5% as the main parameter of use.

Materials and methods

Material

The measured briquettes consisted of the coconut shell charcoal briquettes in three geometric shapes, namely tube, cube, and hexagon, as shown in Fig. 1. The briquettes were products of a factory in Klaten, Central Java, Indonesia. The cube briquettes were 2.5 cm on each edge. The tube briquettes had a diameter of 2.23 cm and a length of 3.91 cm. The hexagonal briquettes featured a cross-sectional area of 4.5 cm^2 with a length of 5

Fig. 1 The cube, tube, and hexagonal briquettes used in this work

cm. In terms of composition, the briquettes was 95% of coconut shell charcoal and 5% of tapioca starch as the binder, as in Anis et al. [41]. The briquettes were made with screw extruder compaction at a ratio of 4:1, resulting in a final specific density of 1.0–1.1 as the regulation required. Subsequently, the drying process was conducted at a temperature of 65 °C and 20% humidity and lasted between 13 and 18 h. The drying duration varied depending on the number of briquettes in every batch.

Measuring resistivity

The measurement equipment to determine the completion duration of the drying process consists of two plate electrodes squeezing measured briquette, and a digital multimeter as shown in Fig. 2. The electrodes were made of PCB and were assisted with an electrolyte of potassium nitrate 3.05%, which was conveyed in a sponge attached directly to the electrodes to increase the contact between the electrodes and the briquette surface. The direct method used an ohmmeter to measure the resistance. Following, the resistivity was calculated using Eq. (1). Then, this measurement was applied under varying moisture content conditions. The indirect method applied a voltmeter to measure the potential difference of the briquettes in a voltage divider circuit, as shown in Fig. 3. Accordingly, Eq. (6) was used to calculate the briquette resistivity. The direct method has

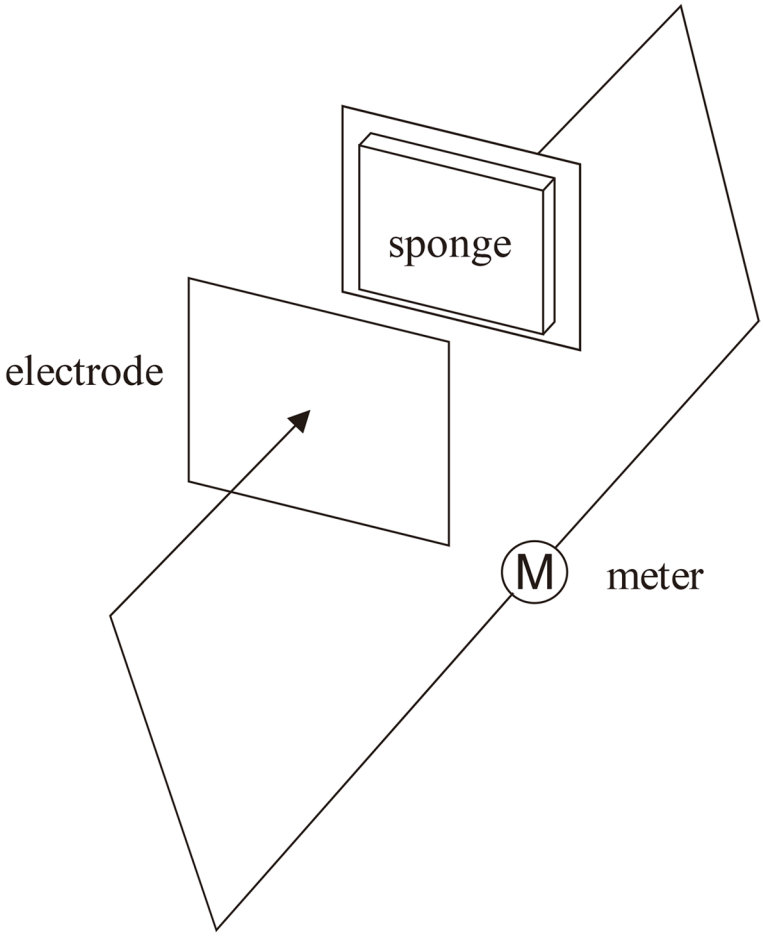

Fig. 2 The structure of equipment for measuring the resistivity

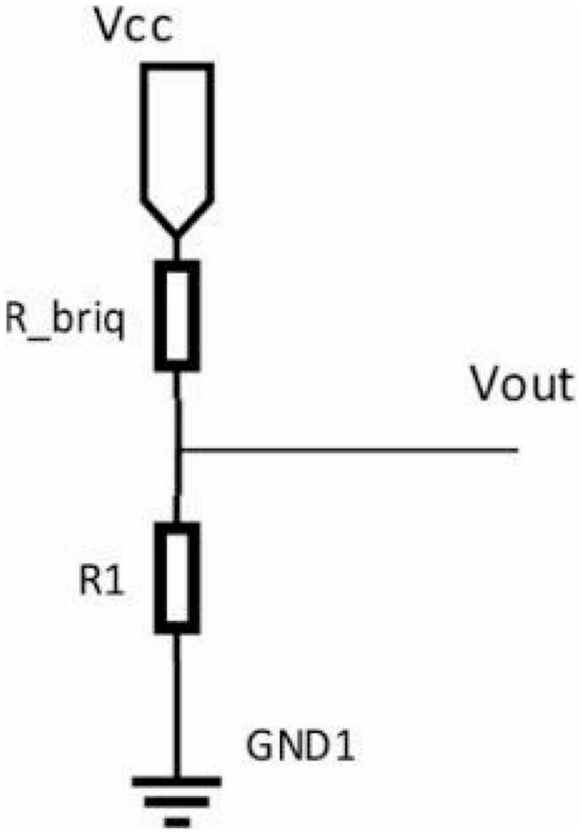

Fig. 3 The voltage divider with the output voltage as the main measured variable and R_briq as the charcoal briquette

an equipment accuracy of 1.5% + 5 with a resolution of 0.1 ohm. Meanwhile, the indirect method exhibited an equipment accuracy of 0.7% + 3 and a resolution of 0.1 mV.

Basic resistivity measurement

Resistivity measurement is based on a resistance measurement. Commonly, the generic function of measurement is shown in Eq. (2), where i represents the current density, defined as the ratio of electric current to cross-sectional area. Meanwhile, E and σ denote the electric field and the conductivity, respectively. The resistivity is the inverse of the conductivity. Therefore, it can be determined using Eq. (1). As shown in this equation, the resistivity (ρ) depends on the cross-sectional area of the material (A), the length of the material (l), and the measured characteristic variable, namely the resistance (R). Thus, Eqs. (1) and (2) indicate that resistivity can be obtained either by measuring the resistance of a material with a known length and cross-sectional area or by calculating it from the measured current density under a specified electric field across the material.

$$\rho = \frac{AR}{l} \tag{1}$$

$$i = \sigma E \tag{2}$$

Equation (1) implies the direct method. An ohmmeter is used to measure the electrical resistance of the briquette. Subsequently, a simple manipulation based on the briquette

dimensions is applied to determine the resistivity of the briquette, following Eq. (1). With plate electrodes, the assumption of cross-section can be used directly.

Equation (2) describes the current measurement approach that demonstrates an indirect measurement method. The current is measured in the wire supplying the potential for the briquette. Whereas, the potential difference between the sides of the briquette is maintained by the electrodes. The primary function of the electrode plate is to create a charge boundary that generates an electric field. The cation has a negative charge along a plate, while the anion creates the boundary of positive charge along the other plate. The dry briquette prevents the ion from moving to the other side. On the contrary, the wet briquette allows the ions to move through the briquette. Consequently, the different drying levels produce different potentials between the electrodes.

Voltage divider

The potential difference between the electrodes can be measured using a voltage divider, which serves as the main sensor element. The voltage divider, coupled with an instrumentation amplifier, is applied to convert the sensor signal into a potential that is used to measure the current. The voltage divider circuit is presented in Fig. 3. The main components of the voltage divider are *R_briq* and *R_1*. The *R_briq* is the resistivity of the briquette, and the *R_1* is selected to be 10 kOhm. The relationship between the R_briq and Vcc is shown in Eq. (3), followed by Eq. (4).

$$I = \frac{Vout}{10\ \mathrm{k}\Omega} \tag{3}$$

$$R\_briq = \frac{Vcc - Vout}{I} \tag{4}$$

Therefore, by applying the relationship in Eq. (1), the resistivity of the briquette can be expressed as Eq. (5).

$$\rho_{briq} = \frac{(Vcc - Vout)\,A}{Il} \tag{5}$$

Then,

$$\rho_{briq} = \frac{(Vcc - Vout)\,A * 10^4}{Vout * l} \tag{6}$$

Equation (6) shows that the resistivity of the briquette is a function of *Vout*, while the other parameters remain constants. Therefore, the measurement method described in Eq. (6) creates an indirect method.

Electrolyte

The electrolyte chosen for resistivity measurement was potassium nitrate. A solution of 2,8 g potassium nitrate in 90 cc of water was applied. The potassium nitrate has been reported to indicate a conductivity of 0,09479 × 10^{-8} S/cm [42]. The conductivity of a weak electrolyte decreases with increasing concentration according to Kohlrausch's law, as mentioned in Eq. (7) [43]

$$A_m = A_0 - bc^{1/2} \tag{7}$$

with Am as the conductivity of a specific concentration, and A_0 as the conductivity of 0 concentration, and C as the concentration of the solution in % of mol. The other variable is the constant.

Procedure

The direct method consisted of setting the meter to ohmmeter mode, adding the electrolyte to the sponge, reading the data, and calculating the resistivity. The amount of the electrolyte added to the sponge was 0.25 ml for each electrode. Then, the resistivity was calculated from the resistance data according to Eq. (2) was performed on the resistance data as the measured variable.

The indirect method followed similar initial steps. The electrodes were connected to a 5 V power supply and arranged in a voltage divider circuit. The meter was set as a voltmeter and connected to the output of the voltage divider. Subsequently, 0.5 ml of electrolyte was added, and the briquette was squeezed between the electrodes. The resistivity was then calculated using Eq. (6).

The direct measurements were performed on 14 cube briquettes with varying moisture content. Resistance measurements were conducted three times for each sample. Averaging of the read data was used as the result. A comparison of the moisture content, density, and resistivity obtained using this method is presented to show that the resistivity method is more effective than the density method in measuring the stopping condition.

The resistivities of the tube briquettes were measured using an indirect method. Eighteen samples of tube briquettes with different moisture content were collected during the drying process. The voltage divider was varied using resistances of 100 Ohm, 1 kOhm, 10 kOhm, and 100 kOhm. Averaging of the resistivity was conducted to obtain the best result. Similarly, the resistivity of the hexagonal briquette samples was also measured using the indirect method with a voltage divider of 100 Ohm, 1 kOhm, 10 kOhm, and 100 kOhm.

Two different conditions of cube briquettes were measured as the final validation of the resistivity method for determining the stop condition of drying. An application of a 10 kOhm divider resistance was used to sense the briquettes' voltage. Then, the digital data acquisition was performed using a microcontroller, with each sample measured 32 times.

The moisture content was measured according to [13]. The samples were put into an oven at a temperature of 105 °C for 1 h. The moisture content was calculated as the ratio of the mass difference between final conditions to the initial mass.

Presentation

The relationship among the parameters obtained from the direct method is presented in pairs. The first pair has a relationship with the moisture content and resistivity, showing resistivity as a function of the moisture content. The second pair relates the mass of the briquette to moisture content, revealing it as a function of mass. The third pair links mass and the resistivity, which explains the potential of using resistivity for moisture content prediction. The relationship of moisture content and resistivities is also applied to tube and cube briquettes to show the similarity of the pattern and the applicability of the method when using an indirect method.

Two briquette conditions of indirect measurement were examined with the focus on the consistency result of the method, regarding the contact between the electrodes and the briquette. The main points of the last indirect method were to show the effect of the electrolyte's conductivity on the measurement and moisture content prediction.

Results and discussions

The use of an electrolyte on a plate electrode for measuring the resistivity is studied in three main steps. The first step is about the conductivity of the electrolyte. It is followed by the direct method as the second step. Parameters, including mass, moisture content, and resistivity, are paired for data at moisture content values ranging from 16% to 4%. The moisture content values were obtained from drying duration of 0–13 h. The discussion explains how each parameter relates to the others. Afterward, the third step discusses the indirect method applied to measure the resistivity of the briquettes under wet and dry conditions. The main focus of this section is to demonstrate the possibility of applying an electrolyte to improve the reliability of the method.

The conductivity of the electrolyte

The conductivity of the potassium nitrate, used as the electrolyte in this research, is determined by extrapolating potassium nitrate solution data according to CRC Handbook of Physics and Chemistry, as shown in Fig. 4 [44]. Equation (7) indicates that the conductivity of a specific potassium nitrate concentration can be obtained using a logarithmic function, applying the trendline of the potassium nitrate solution. The specific conductivity of the applied potassium nitrate in the research was 45.75 S/m. This value was calculated from the data presented in Fig. 4 using the solution concentration in molar and the parameter A in m^2 mS mol^{-1}. For a briquette with a length of 2.5 cm, the solution exhibits a current density of 5.72 A m^{-2} when a 5 V potential is applied between the electrodes. In each measurement, only 0.5 ml of potassium nitrate solution was added, resulting in a current capacity of 1.14×10^{-4} A. This condition corresponds to an

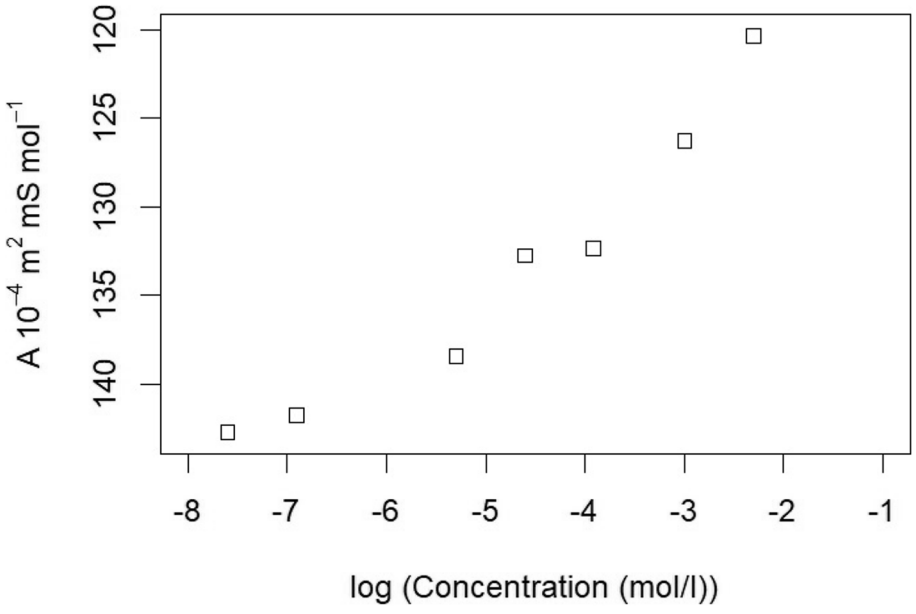

Fig. 4 Higher concentration shows less conductivity

equivalent resistance of 4.37×10^4 Ω. This value represents the resistance of the solution contributing to the total resistance of the briquette.

An electrolyte solution diffused within a briquette can be modelled as the parallel resistance of the briquette and the solution. This model is applied in the capillary bundle model used in rock formation analysis [45]. A dry charcoal briquette has a resistivity of 0.182 MΩm [28, 32]. It means that a cube carbon briquette with a length of 2.5 cm has a resistance of 7.3 MΩ. Therefore, the dry briquette resistance is significantly higher than the resistance of the electrolyte solution.

The dry briquette with fully diffused solution will have a resistance of 4.34 10^4 Ω. In contrast, the wet briquette with a resistivity of 232 Ωm shows 9.30 10^3 Ω resistance [32]. Similarly, the resistance for a fully diffused solution briquette is 7.66 10^3 Ω. The difference between the dry and wet briquettes is significant, and it has the potential to determine the briquette condition if the solution diffuses into the briquette. Even though the resistance of the electrolyte lies between the dry and wet, it still provides a significant distinction between the dry and wet briquettes. For the dry briquette, the electrolyte resistance is dominant. Meanwhile, the wet briquette resistance becomes dominant during the measurement.

Direct measurement

The direct method applied to measure the effect of the moisture content on the briquette resistivity shows an increase in the resistivity as the moisture content decreases, as shown in Fig. 5. The data can be grouped into 3 clusters: the briquettes with moisture content below 5%, the briquettes with moisture content between 6% and 8%, and the briquettes with moisture content greater than 8%. The briquettes with the moisture content below 5% exhibit resistivity values higher than 20 kOhm m. The results confirm the findings of previous work by Prasetyadi et al. [28, 32]. Higher resistivity of the briquette indicates lower moisture content of the briquette. To be a good briquette, the proper agglomeration process should happen in the briquette, which implies higher resistivity.

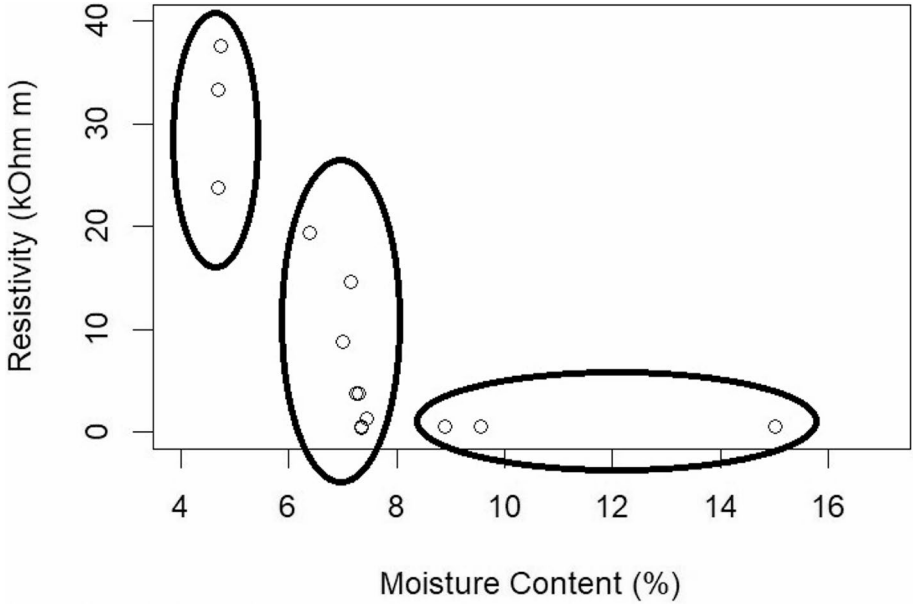

Fig. 5 The resistivity as function of moisture content

Conversely, the briquettes with moisture content of 8% or higher show resistivity values lower than 1 kΩm and therefore do not meet the Indonesian and Japanese standards. The number indicates a wet briquette condition according to the model.

As seen in Fig. 5, the resistivity of the briquette changes significantly as the moisture content decreases from 8% to 4%. A moisture content of 8% or higher indicates that the water content is distributed almost evenly throughout the briquette. Meanwhile, the coconut charcoal briquette with an moisture content below 8% do not contain enough water, which is equally distributed over the briquette. Hence, the briquettes with moisture content below 8% can be considered unsaturated, while those above 8% may be regarded as saturated. The phenomenon observed in Fig. 5 is similar to that of porous rock, in which resistivity decreases exponentially in unsaturated conditions [46]. At the same time, the briquette with moisture content below 8% has lost more than half of the water mass. According to moisture content calculation procedure, the mass change should have a linear relationship with the moisture content. The mass difference is proportional to the moisture content, with the mass factor acting as the coefficient. However, the mass difference has a less significant influence on moisture content than resistivity, which exhibits an exponential relationship with moisture content under unsaturated conditions.

Mass-moisture content relation

Generally, the mass of the briquette decreases as the moisture content becomes lower. As shown in Fig. 6, below 8% moisture content, the mass shows a less significant response to differences in moisture content compared to conditions above this level. The trend of the graph tends to follow a positive exponential pattern. This implies that adjusting moisture content using density for briquettes below 8% is difficult. This finding confirms the authors' previous works [28] and [32]. Nevertheless, briquettes with a mass below 15 g ensure moisture content under 6%. This condition meets the briquette requirements reported in [4, 6, 25, 32, 47, 48].

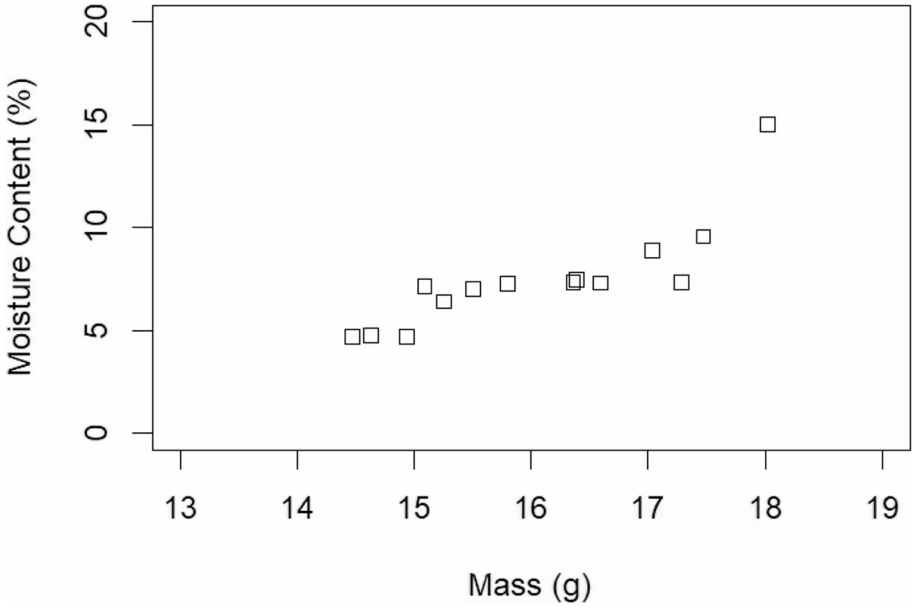

Fig. 6 Mass of the briquettes and their moisture content

The moisture content of the briquettes strongly depends on the drying process. To remove moisture inside the briquette, a thermal process is required to evaporate water from the briquette's pores. Evaporation typically begins at the surface of the briquette, leaving the most difficult-to-remove moisture in the centre of the briquette [20]. The study also reported that the briquette temperature becomes equal to the ambient temperature within one hour. This implies that mass transfer processes influence the temperature distribution inside the material. The temperature difference between the surface and the inner part of the briquette also depends on its moisture content. This process underlines the internal binding mechanism of the briquette during evaporation. Particle size also contributes to this process and creates a trade-off. Fine particles require more water to agglomerate [49]; however, they allow better compaction, which affects the density and strength of the briquette [23]. This emphasizes the importance of studying particle size effects, as highlighted in Pang et al. [50].

Mass-resistivity relation

Figure 7 shows how the resistivity of the briquettes varies with the mass. The relationship is of a negative exponential nature as mass decreases, resistivity increases. This exponential relationship is more significant at lower mass levels. It shows that even a reduction of mass, in this case indicative of moisture content, increases resistivity substantially. This high sensitivity means that measuring resistivity will be much easier to track changes in moisture content than directly weighing the sample. Because of this significant sensitivity, the tracking of moisture content drops below levels of 8% is particularly notable. This makes resistivity excellently suited to track the drying process. As mass decreases towards the required level of dryness, the exponential nature of the relationship ensures that the measured value will become exponentially more significant, providing a good indicator of the later stages of the drying process.

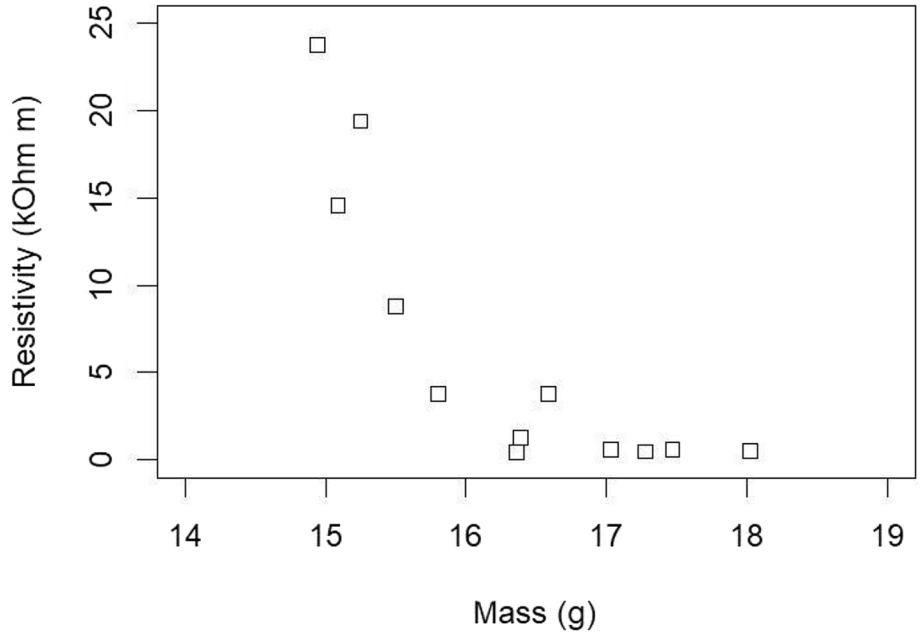

Fig. 7 Resistivity and mass relation of the briquette during the drying process

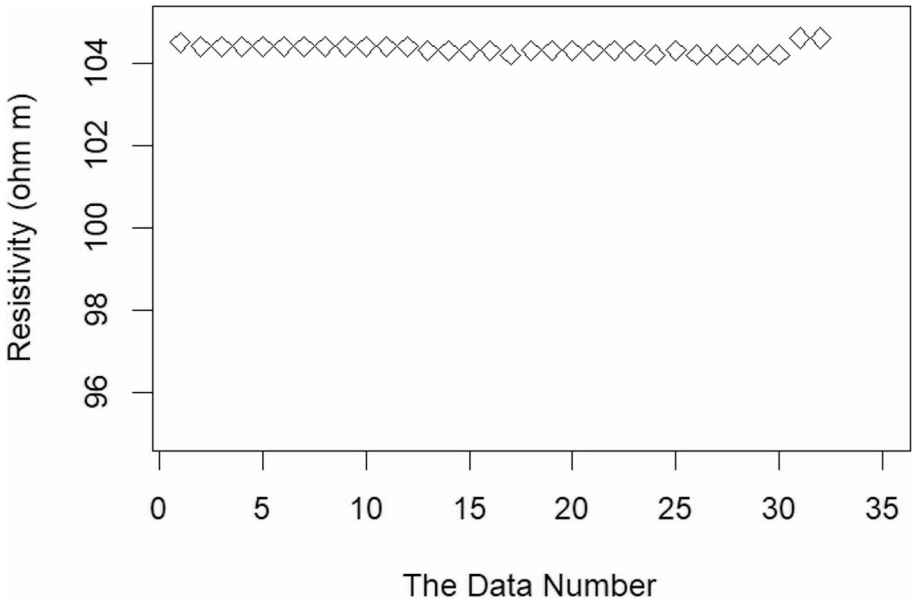

Fig. 8 The data distribution of wet briquette resistivities of the indirect method

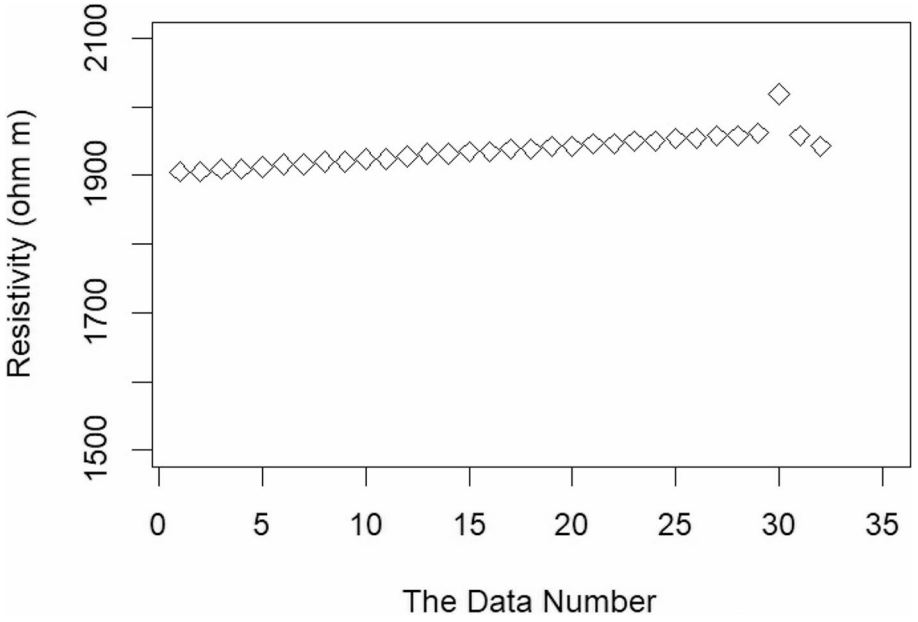

Fig. 9 The data distribution of dry briquette resistivities of the indirect methods

Resistivity measurement using an indirect approach

Resistivity of the wet briquette was measured in 21 s for every sample, and the sampling range was 0.7 s. The results of the sample measurement are shown in Figs. 8 and 9 for wet and dry, respectively. The graphs indicate that the resistivity derived from the indirect calculation method is reasonable in relation to the close range of data. The wet briquette provided adequately consistent data. The data appears to be varied, but that is due to rounding of the bits, resulting in a variation of at most 1%. The average resistivity measured from a total of 12 samples of the wet briquette, using the plate electrodes and indirect method, is 109.5 ± 3.7 Ωm. This is significantly lower than the theoretical

resistivity of wet briquettes, which is 232 Ωm. The resistivity measured of the wet briquettes is below 5%.

Similar results can be observed for the dry briquette, as shown in Fig. 9. There is a significant difference between the wet and dry briquettes. The theoretical dry resistivity should be approximately 43.4 kΩm. The measured resistivity of the dry briquettes is approximately 1937 ± 23 Ωm. Similar to the wet briquettes, the resistivity of the dry briquette standard deviation is less than 5%.

The difference is attributed to the diffusion of the electrolyte. As the sensor measures the voltage, the resistive sensing comes into play. This sensor comes with a built-in impedance, which lowers the measured output voltage and, in turn, lowers the measured resistivity. If the sensor is assumed to have an 80 kΩ impedance, the theoretical calculation on the sensor should indicate the resistivity of the dry briquette to be approximately 1.9 kΩ m. For the wet briquette, the conditions were different because some of the electrolyte was absorbed by the briquette, which altered the resistivity of the briquette. This caused the wet briquette resistivity to be lower. Considering the same sensor impedance, the resistivity of the wet briquette is approximately 116 Ωm.

The changes in resistivity of the briquettes due to diffusion of the electrolyte, at the same time, explain the difference in conditions of the briquettes. Mass and resistivity are influenced by electrolyte diffusion. The mass change affecting moisture content from the 1st cluster (below 5%) to the 2nd cluster (between 5% and 8%) implies resistivity of the measured dry briquette. The resistivity is still higher than 1 kΩm. The wet briquette is also affected by the electrolyte diffusion, with the reducing of the resistivity. The wet and the dry briquettes can still be distinguished.

The resistivity of the briquettes can be read using a microcontroller and can be done in less than one minute. The result can be used to determine the drying finish judgment. The process is faster than conventional methods such as the proximity approach and burning test. The methods consume 1 h and 3 h for the proximity and burning test, respectively. The resistivity method can reduce fuel consumption by 2% and 5% for the proximity and burning test, respectively.

Different shapes of briquettes resistivity indirect approach

The indirect approach was applied to tube-shaped and hexagonal-shaped briquettes under various moisture content conditions. Figures 10 and 11 show the trends of the resistivity as a function of moisture content for tube-shaped and hexagonal-shaped briquettes, respectively. The resistivity data were collected 4 times for every moisture content with the different stagger resistors as mentioned previously. The deviational standards of the collected resistivity data are less than 1.5%. In Fig. 10, briquettes' resistances are linear with the moisture content 4 to 6%. Figure 11 talks about the resistances of hexagonal-shaped briquettes of 3 to 10% moisture content. The resistivity of the graph of the cube-shaped briquettes 4 to 16% moisture content also presents a lot of similarity with both graphs. The graphs show some consistent patterns. In the range of 4 to 6% moisture content, the resistivity tends to vary significantly. The resistivity of the briquettes below 5% moisture content are for the most part, relatively high (greater than 10 kOhm m) compared to the moisture content above 5%. It also shows the possibility of using resistivity as the moisture content determinant for different charcoal briquettes with some adjustment based on their density and carbon composition.

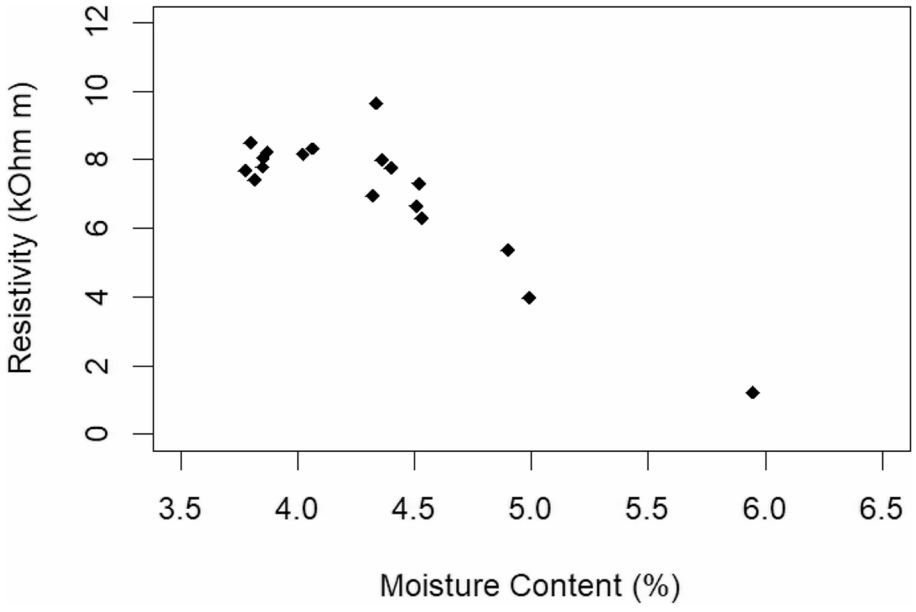

Fig. 10 The resistivity of tube-shaped briquettes for various moisture content

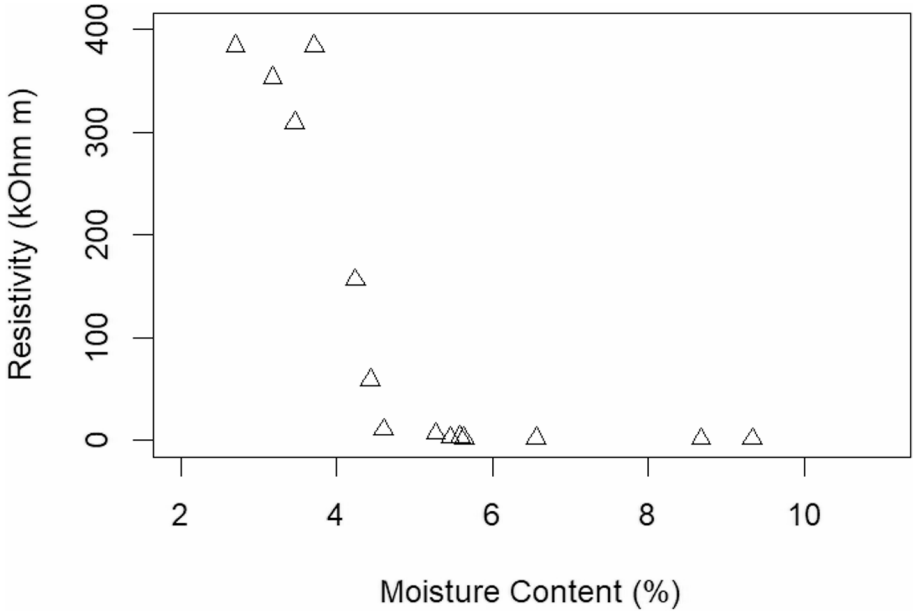

Fig. 11 The resistivity of hexagonal-shaped briquettes for various moisture content

Further calibration studies are still required to reduce the uncertainty of the threshold. Several parameters related to electrolyte diffusion influence resistivity. In addition, the dimensions of the briquettes affect electrolyte adsorption and its impact on the material's electrical conduction.

The uncertainty of the measurement

The proposed method works with some limitations. For the contact probe of equipment operating with a sensitivity of 0.1 V, the uncertainty has to be taken into consideration. For a cube-shaped briquette of 2.5 cm edge length, the sensitivity can yield 9.23 kohm

m for a 10 kohm stagger resistant of the voltage divider. The balance between the equipment sensitivity and the skill-dependent uncertainty ought to be taken into consideration for measurements near the voltage limit. It is preferable to keep the voltage within the 1/3 center range.

Conclusion

Both direct and indirect methods can be used to measure resistivity using a potassium nitrate solution measuring 45.75 mS/cm. The direct methods focus on potential resistivity and moisture content determination. The indirect methods show consistent resistivity of the briquette in every measurement. The results were consistent with low standard deviations (under 5%). The consistent measurements of resistivity suggest that the method used to measure the resistivity of charcoal is reliable. This means that the conductive plate electrodes and charcoal can identify the dry and ready-to-use state during the manufacture of charcoal briquettes, fulfilling the aim of the research. As the water content (MC) decreases below 6%, the resistivity increases significantly.

Briquettes with a moisture content exceeding 6% have resistivity of less than 1 kΩ m, whereas briquettes with moisture content below 5% have resistivity exceeding 10 kΩ m. This range of moisture content is desirable for briquettes in the marketplace, so resistivity measurements on briquettes can be used to estimate the moisture content and can also be used to measure when the drying process is finished. The application of resistivity also allows for a reduction in the time taken to identify the completion point for drying coconut charcoal briquettes. Additionally, the method can also reduce fuel consumption by 5% for the conventional burning test.

Acknowledgements

The Authors express their gratitude to DRTPM - Kementerian Riset, Teknologi dan Pendidikan Tinggi Republik Indonesia (Ministry of Research, Technology, and Higher Education of Indonesia) to provide financial support for the research leading to the work through the 2024 Fund.

Authors' contributions

Andreas Prasetyadi: Conceptualization, methodology, formal analysis, writing original draft, project administration, validation, Bernadeta Wuri Harini: responsible to provide instrument to measure the resistivity using a microcontroller and conducting measurements using a microcontroller, Rusdi Sambada: preparing the graphics and table, review and editing. All authors have read and agreed to the published version of the manuscript.

Funding

This research was funded by DRTPM (Direktorat Riset Teknologi dan Pengabdian kepada Masyarakat) of the Ministry of Research, Technology, and Higher Education of Indonesia with contract No. 107/ES/ PG.02.00.PL/2024, No. 0609.11/LL5-INT/AL.04/2024, and 035 Penel./LPPM-USD/VI/2024.

Data availability

Data sharing is not applicable as no datasets were generated.

Declarations

Competing interests

The Authors declare that the work is original and has not published in any other journal nor in consideration for any publication.

Received: 11 October 2025 / Accepted: 16 March 2026

Published online: 19 March 2026

References

1. Ameer K, Shahbaz HM, Kwon JH (2017) Green extraction methods for polyphenols from plant matrices and their byproducts: a review. Compr Rev Food Sci Food Saf 16(2):295–315. https://doi.org/10.1111/1541-4337.12253
2. Gunawan S, Nursanni B, Suprapto, Januariyansah S (2022) The utilization of biomass waste as charcoal briquette to reduce waste disposal. In: Journal of Physics: Conference Series. Institute of Physics. https://doi.org/10.1088/1742-6596/2193/1/012086

3. Khan AU, Jan QMU, Abas M, Muhammad K, Ali QM, Zimon D (2023) Utilization of Biowaste for Sustainable Production of Coal Briquettes. Energies 16(20). https://doi.org/10.3390/en16207025
4. Garrido MA, Conesa JA, Garcia MD (2017) Characterization and production of fuel briquettes made from biomass and plastic wastes. Energies 10(7). https://doi.org/10.3390/en10070850
5. Roman K, Rzodkiewicz W, Hryniewicz M (2023) Analysis of forest biomass wood briquette structure according to different tests of density. Energies 16(6). https://doi.org/10.3390/en16062850
6. Siharath P et al (2024) The calorific value experiment on coconut shell, bamboo and mixed charcoal briquette. Asian J Sci Technol Eng Art 2(1):83–92. https://doi.org/10.58578/ajstea.v2i1.2480
7. Oyelaran OA, Bolaji BO, Waheed MA, Adekunle MF (2015) Performance evaluation of the effect of binder on groundnut shell briquette. KMUTNB Int J Appl Sci Technol 8(1):11–19. https://doi.org/10.14456/kkuenj.2015.32
8. Oyelaran OA, Bolaji BO, Waheed MA, Adekunle MF (2015) An experimental study of the combustion characteristics of groundnut shell and waste paper admixture briquettes. Artic KKU Eng J 42(4):283–286. https://doi.org/10.14456/kkuenj.2015.32
9. Oyelaran OA, Bolaji BO, Waheed MA, Adekunle MF (2015) Characterization of of briquettes produced from groundnut shell and waste paper admixture. Iran J energy Environ 6(1). https://doi.org/10.5829/idosi.ijee.2015.06.01.07
10. Saneewongnaayutaya N, Khamdaeng T, Panyoyai N, Tippayawong N, Wongsiriamnuay T (2022) Production and Characterization of Fuel Briquettes from Rice Husks and Tobacco Stalks. In: AIP Conference Proceedings. American Institute of Physics Inc. https://doi.org/10.1063/5.0115139
11. Niño A, Arzola N, Araque O (2020) Experimental study on the mechanical properties of biomass briquettes from a mixture of rice husk and pine sawdust. Energies 13(5). https://doi.org/10.3390/en13051060
12. Mencarelli A, Cavalli R, Greco R (2022) Variability on the energy properties of charcoal and charcoal briquettes for barbecue. Heliyon 8(8). https://doi.org/10.1016/j.heliyon.2022.e10052
13. Nikiforov A, Kinzhibekova A, Prikhodko E, Karmanov A, Nurkina S (2023) Analysis of the characteristics of bio-coal briquettes from agricultural and coal industry waste. Energies 16:8. https://doi.org/10.3390/en16083527
14. Handra N, Hafni H (2017) Effect of Binder on Combustion Quality on EFB Bio-briquettes. In: IOP Conference Series: Earth and Environmental Science. Institute of Physics Publishing. https://doi.org/10.1088/1755-1315/97/1/012031
15. Lestari L, Variani VI, Firihu MZ, Raharjo S, Saleh I, Aprilla N (2020) Effect of compaction pressure on quality of activated charcoal briquette made from Sago Stem Midrib Material. In: IOP Conference Series: Materials Science and Engineering. Institute of Physics Publishing. https://doi.org/10.1088/1757-899X/797/1/012022
16. Obi OF, Pecenka R, Clifford MJ (2022) A Review of biomass briquette binders and quality parameter. MDPI. https://doi.org/10.3390/en15072426
17. Sanchez PD, Aspe MMT, Sindol KN (2022) An overview on the production of bio-briquettes from agricultural wastes: methods, processes, and quality. J Agric Food Eng 3(1):1–17. https://doi.org/10.37865/jafe.2022.0036
18. Tanui JK, Kioni PN, Kariuki PN, Ngugi JM (2018) Influence of processing conditions on the quality of briquettes produced by recycling charcoal dust. Int J Energy Environ Eng 9(3):341–350. https://doi.org/10.1007/s40095-018-0275-7
19. Adam SNFS, Aiman JHM, Zainuddin F, Hamdan Y (2021) Processing and characterisation of charcoal briquettes made from waste rice straw as a renewable energy alternative. In: Journal of Physics: Conference Series. Institute of Physics. https://doi.org/10.1088/1742-6596/2080/1/012014
20. Paul G, Olivier M, Esther A, Daniel M, Jean CL (2019) Heat and mass transfer local modelling applied to biomass briquette drying. In: Procedia Manufacturing. Elsevier B.V., pp 149–154. https://doi.org/10.1016/j.promfg.2019.05.018
21. Njenga M Challenges and opportunities for charcoal briquette enterprises in East Africa. Available: https://www.researchgate.net/publication/352561574. Accessed 20 May 2024
22. Sundari N, Papuangan, Jabid AW (2019) Pre-design of bio-briquette production using Kenari Shell. In: IOP Conference Series: Earth and Environmental Science. Institute of Physics Publishing. https://doi.org/10.1088/1755-1315/276/1/012051
23. Dalimunthe YK, Widayani, Aditya ID (2023) Briquettes optimization of palm shell waste and LDPE plastic based on particle size and compressive strength as alternative fuels. In: IOP Conference Series: Earth and Environmental Science. Institute of Physics. https://doi.org/10.1088/1755-1315/1239/1/012017
24. Ma O (2020) Combustion characteristics of high-density briquettes produced from sawdust admixture and its performance in briquette stove combustion characteristics of high-density briquettes. https://doi.org/10.13140/RG.2.2.12104.55044
25. Marreiro HMP, Peruchi RS, Lopes RMBP, Andersen SLF, Eliziário SA, Junior PR (2021) Empirical studies on biomass briquette production: a literature review. MDPI. https://doi.org/10.3390/en14248320
26. Rodriguez PG, Annamalai K, Sweeten J (1998) The effect of drying on the heating value of biomass fuels, transactions of the ASABE. 41(4):1083–7. Available from: https://elibrary.asabe.org/abstract.asp?aid=17237
27. Sunardi S, Djuanda D, Mandra MAS (2019) Characteristics of charcoal briquettes from agricultural waste with compaction pressure and particle size variation as alternative Fuel. Int Energy J 19:139–148
28. Prasetyadi A, Sambada R, Purwadi PK (2024) Development of a new fast drying determinant method using resistivity for the industry of coconut shell charcoal briquettes. Eastern Eur J Enterp Technol 1(127):58–66. https://doi.org/10.15587/1729-4061.2024.297541
29. Demirbas A (2002) Relationships between heating value and lignin, moisture, ash and extractive contents of biomass fuels. Energy Explor Exploit 20(1):105–111
30. Gebreegziabher T, Oyedun AO, Hui CW (2013) Optimum biomass drying for combustion - a modeling approach. Energy 53:67–73. https://doi.org/10.1016/j.energy.2013.03.004
31. Madyira DM (2014) Biomass briquette drying process using solar energy
32. Prasetyadi A, Sambada R, Purwadi PK (2024) Alternative method for stopping the coconut shell charcoal briquette drying process. In: E3S Web of Conferences. EDP Sciences. https://doi.org/10.1051/e3sconf/202447501007
33. Asamoah B, Nikiema J, Gebrezgabher S, Odonkor E, Njenga M (2016) A review on production, marketing and use of fuel briquettes. Colombo Sri Lanka. https://doi.org/10.5337/2017.200
34. Prasetyadi A, Sambada FAR, Harini BW (2025) The mass time burning model of coconut shell charcoal briquettes. Eng Headw 18:93–98
35. Cromarty R, Bharat S, Odendaal D (2023) Electrical resistivity of heat-treated charcoal correspondence to: dates: how to cite. J South Afr Inst Min Metall 123(10):501–508. https://doi.org/10.17159/2411

36. Xiao G, Xiao R, Jin B, Zuo W, Liu J, Grace JR (2010) Study on electrical resistivity of rice straw charcoal. J Biobased Mater Bioenergy 4(4):426–429. https://doi.org/10.1166/jbmb.2010.1093
37. Токторбаева ГП (2022) Determination of specific electrical resistance of walnut charcoal. Sci Herit 2006:116–120. https://doi.org/10.5281/zenodo.6696562
38. Harini BW, Sambada R, Muda VHP, Prasetyadi A (2025) Drynesslevel measurement of coconut shell charcoal briquettes using plate shaped electrodes. In: NST Proceeding 1st International Conference onIndustrial Electronics, Robotics and Informatics:1–9. https://doi.org/10.11594/nstp.2025.5101
39. RevilA, Jardani A (2013) The self-potential method: theory and applications in environmental geosciences. Cambridge University Press. https://doi.org/10.1017/CBO9781139094252
40. Huroeroh A, Anggita SR, Kusuma HH (2021) Analysis of moisture content, calorific value and burning rate of Corncob and Kopok Randu (Ceiba pentranda) skin briquette. Al-Fiziya J Mater Sci Geophys Instrum Theor Phys 4(1):21–28. https://doi.org/10.15408/fiziya.v4i1.19745
41. Anis S et al (2023) Effect of adhesive type on the quality of coconut shell charcoal briquettes prepared by the screw extruder machine. 1–16. https://doi.org/10.32604/jrm.2023.047128
42. Haynes WM, Lide DR, Bruno TJ (2017) CRC Handbook of chemistry and physics, 97th edn
43. Walsh FC (1992) Electrolytic conductivity and its measurement. Trans Inst Met Finish 70(1):45–49. https://doi.org/10.1080/00202967.1992.11870940
44. Vany´sek PV (2012) Equivalent Conductivity of Electrolytes in Aqueous Solution. In: CRC Handbook of Chemistry, and Physics, 93th edn. Taylor & Francis, pp. 5–74
45. Zhu L, Wu S, Zhang C, Misra S, Zhou X, Cai J (2023) Characterization of pore electrical conductivity in porous media by weakly conductive and nonconductive pores. Springer Sci Bus Media B V https://doi.org/10.1007/s10712-022-09761-w
46. Park SG, Shin SW, Lee DK, Kim CR, Son JS (2016) Relationship between electrical resistivity and physical properties of rocks. In: 22nd European Meeting of Environmental and Engineering Geophysics, Near Surface Geoscience 2016. European Association of Geoscientists and Engineers, EAGE. https://doi.org/10.3997/2214-4609.201602101
47. Amrullah A, Syarif A, Fauzianur A (2021) Assessment of combustion behaviour of carbonize bio-briquette wood residue under different pressure and particle size. IOP Conf Ser Mater Sci Eng 1034(1):012080. https://doi.org/10.1088/1757-899x/1034/1/012080
48. Sunardi S, Djuanda D, Mandra MAS (2019) Characteristics of charcoal briquettes from agricultural waste with compaction pressure and particle size variation as alternative fuel. Int Energy J 19:139–148
49. Özer M, Basha OM, Morsi B (2017) Coal-agglomeration processes: a review. Int J Coal Prep Util 37(3):131–167. https://doi.org/10.1080/19392699.2016.1142443
50. Pang L, Yang Y, Wu L, Wang F, Meng H (2019) Effect of particle sizes on the physical and mechanical properties of briquettes. Energies 12(19). https://doi.org/10.3390/en12193618

Publisher's note